

# PWM and PFM Controlled Buck Converter designed for Wearable Electronic Devices

Tihomir Brusev<sup>1</sup>, Georgi Kunov<sup>2</sup> and Elissaveta Gadjeva<sup>3</sup>

**Abstract** – Integrated Pulse-Width Modulation (PWM) and Pulse-Frequency Modulation (PFM) controlled buck converter is proposed in this paper, designed for wearable electronic devices. The input voltage is equal to 3.6V and the average value of the output voltage is regulated to be 1.7V. The maximum efficiency  $\eta$  of the buck converter is 81.43%, when the load current  $I_{Load}$  is equal to 68mA. When  $I_{Load}$  is smaller than 8mA the efficiency of the PFM controlled buck converter is around 7% higher compared to the efficiency of the PWM controlled buck converter.

**Keywords** – Buck converters, Pulse-Width Modulation (PWM), Pulse-Frequency Modulation (PFM), Integrated circuits, Cadence.

## I. INTRODUCTION

Today, the number of wearable electronic devices incorporated in the Internet of Things (IoT) systems is growing very fast.

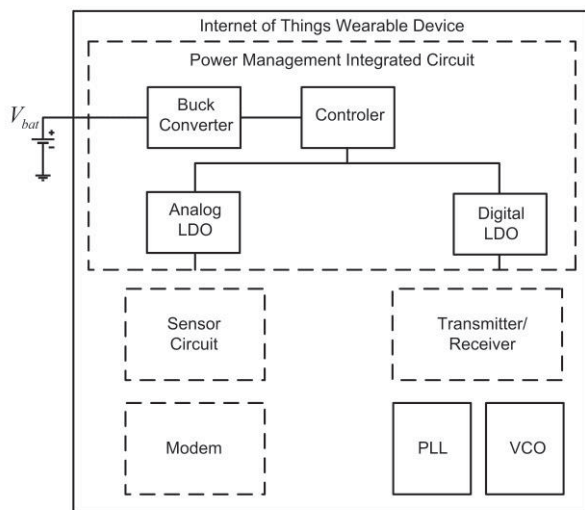


Fig. 1. Block diagram of power management integrated circuit (PMIC) in IoT wearable device [5].

Most of them are battery powered or they use energy from harvesting power sources [1], [2]. Long battery life is required

<sup>1</sup>Tihomir Brusev is with the Faculty of Telecommunications, Technical University of Sofia, Kl. Ohridski 8, 1797 Sofia, Bulgaria, E-mail: brusev@ecad.tu-sofia.bg.

<sup>2</sup>Georgi Kunov is with the Faculty of Electronic Engineering and Technologies, Technical University of Sofia, Kl. Ohridski 8, 1797 Sofia, Bulgaria, E-mail: gkunov@tu-sofia.bg.

<sup>3</sup>Elissaveta Gadjeva is with the Faculty of Electronic Engineering and Technologies, Technical University of Sofia, Kl. Ohridski 8, 1797 Sofia, Bulgaria, E-mail: egadjeva@tu-sofia.bg.

for many portable applications [3]. High efficient buck dc-dc converter integrated together with wearable electronic devices is necessary to be designed and implemented [4]. The block diagram of power management integrated circuit (PMIC) of IoT wearable device is shown in Fig. 1 [5]. The input voltage of the buck converter is equal to 3.6V, while the average output voltage is controlled to be equal to 1.7V [5]. On the other hand the output voltage of switching-mode converter is supply voltage for low drop regulators (LDO), which are shown in Fig. 1. The monolithic buck converter is necessary to occupy small silicon area and respectively to have small external filter inductor and capacitor components [6].

The PWM controlled integrated buck converter designed on CMOS 0.35  $\mu\text{m}$  technology for IoT wearable device is presented in Section II. PFM control of the switching-mode regulator is proposed and presented in Section III. The efficiency  $\eta$  of the designed circuits, when both control techniques are used, is investigated as a function of the load current  $I_{Load}$ . The received results are compared and analyzed.

## II. PWM CONTROLLED BUCK CONVERTER

The PWM controlled buck converter is designed for IoT wearable device with Cadence on CMOS 0.35  $\mu\text{m}$  technology. The block circuit diagram is shown in Fig. 2.

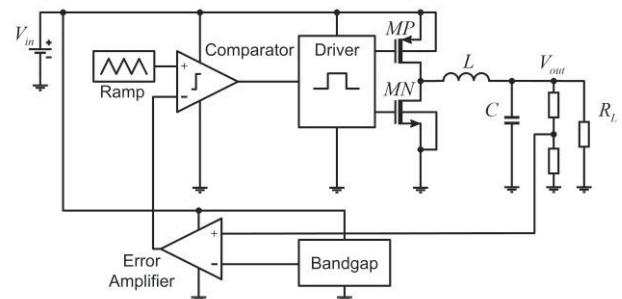


Fig. 2. Block diagram of PWM controlled buck converter.

The input voltage of the switching-mode regulator is equal to 3.6V and the average value of the output voltage is controlled to be equal to 1.7V [5]. The control system includes bandgap voltage reference, error amplifier, ramp generator and driver. The signal, which regulates the states of buck converter's power MOS transistors, is generated by comparing the voltage with repetitive waveform and error control voltage. The error signal is obtained, when difference between the actual output voltage of the whole system  $V_{out}$  and the output voltage level of bandgap reference is amplified. The frequency of the ramp generator defines the switching frequency  $f_s$  of buck converter. This frequency is constant for PWM control technique. The output signal of comparator controls the states of power buck

converter's switches. The schematic of ramp generator is presented in Fig. 3.

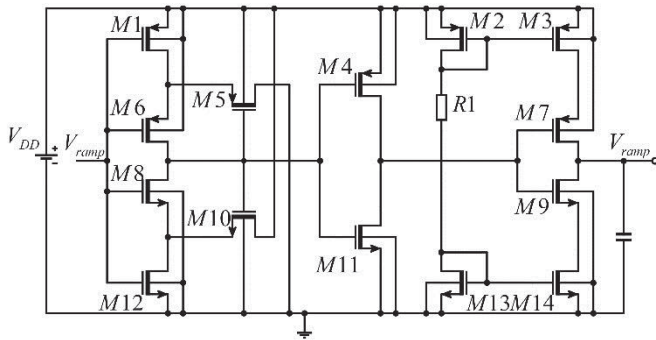


Fig. 3. Ramp generator.

The output stage of the ramp generator consists of two current mirrors. They define the charging and discharging current of the output capacitor  $C_I$ . The switching frequency  $f_s$  of the buck converter depends on the ramp capacitor's value and the current which flows through this component. The waveforms of the output signals of error amplifier, ramp generator and comparator are presented in Fig. 4.

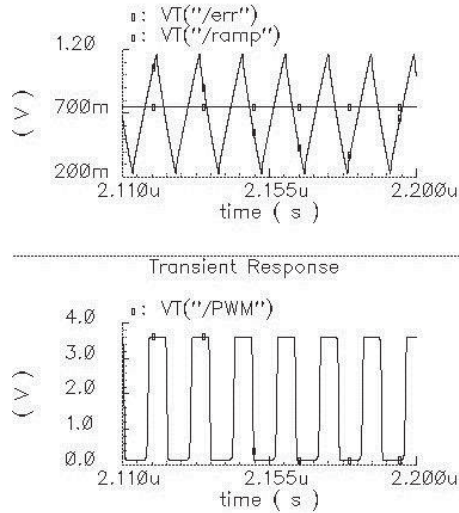


Fig. 4. The waveforms of the output signals of error amplifier, ramp generator and comparator.

The switching frequency  $f_s$  of the designed PWM controlled buck converter is equal to 80MHz.

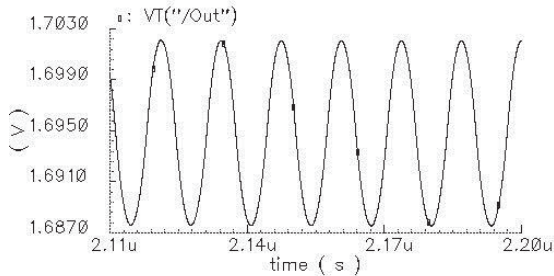


Fig. 5. The waveform of output voltage  $V_{out}$  of the designed PWM controlled buck converter.

The waveform of output voltage  $V_{out}$  of the designed PWM controlled buck converter is shown in Fig. 5. The values of the

filter inductor  $L$  and capacitor  $C$ , which are used in the low-pass filter, are equal to 250nH and 5nF respectively. The efficiency  $\eta$  of the buck converter as a function of the load current  $I_{Load}$  is investigated. The simulated results are presented in Table I.

TABLE I  
PWM CONTROL  
EFFICIENCY OF BUCK CONVERTER AS A FUNCTION OF  $I_{LOAD}$

PWM Controlled Buck Converter	
$I_{Load}$ [mA]	Efficiency [%]
100	75.6
80	80.64
68	81.43
50	80.81
30	79.07
20	74.69
10	62.04
8	56.9
5	45.7
2	28
1	17

The efficiency of the switching-mode regulator is calculated by formula:

$$\eta = \frac{P_{out}}{P_{in}}, \quad (1)$$

where  $P_{out}$  is the average output power and  $P_{in}$  is the average input power of the circuit. The maximum efficiency of the PWM controlled buck converter is equal to 81.43%, when the load current is equal to 68mA. As it can be seen from the received results presented in Table I, the efficiency of PWM controlled buck converter is decreasing at light loads.

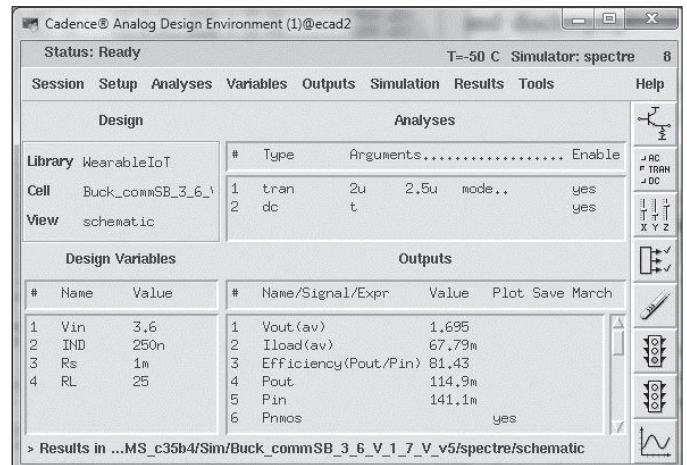


Fig. 6. Simulation results received in Cadence Virtuoso Analog Design Environment when  $I_{Load}=68$ mA.

The simulation results obtained in Cadence Virtuoso Analog Design Environment tool, when the investigated circuit indicates the highest efficiency result, are presented in Fig. 6 [7]. The output power of the converter in this particular case is equal to 115mW.

### III. PFM CONTROLLED BUCK CONVERTER

The PFM controlled buck converter is designed with Cadence on CMOS 0.35  $\mu\text{m}$  technology and the block diagram of the whole system is shown in Fig. 7. The input voltage of the buck converter is equal to 3.6V, while the output voltage is equal to 1.7V. The control system includes bandgap voltage reference, comparator with hysteresis, oscillator and driver stages. The power MOS transistors are regulated by oscillator with fixed 50% duty-cycle. When the actual output voltage of buck converter is higher than the desired level the control system works in sleep mode. In this case the load energy is delivered by filter capacitor  $C$ . The only stages which operate at sleep mode of the converter are bandgap and comparator with hysteresis. When the buck converter works in sleep mode of operation driver, oscillator and the power stage are disabled. Thus power losses in control system are minimized in light load conditions.

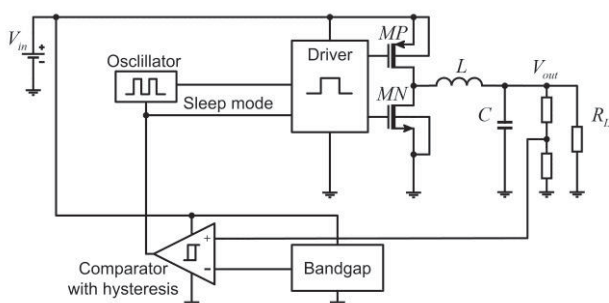


Fig. 7. Block diagram of PFM controlled buck.

The same bandgap voltage reference is used in this control as in the PWM controlled buck converter. If the output voltage  $V_{out}$  becomes smaller than the certain level, the comparator with hysteresis wakes up the whole system. This is the normal mode of operation of the switching-mode regulator. In the pictures bellow the operation of PFM controlled buck converter is presented at different load conditions.

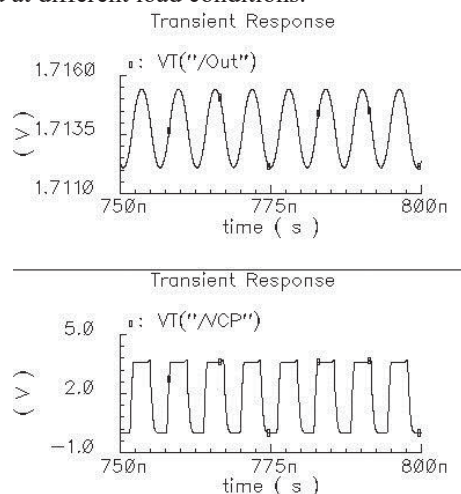


Fig. 8. The waveforms of  $V_{out}$  and control pulses of main power PMOS transistor  $V_{cp}$  when  $I_{Load}=8$  mA.

The waveforms of output voltage  $V_{out}$  and control pulses of main power PMOS transistor  $V_{cp}$ , when the load current  $I_{Load}$  is equal to 8mA, are presented in Fig. 8.

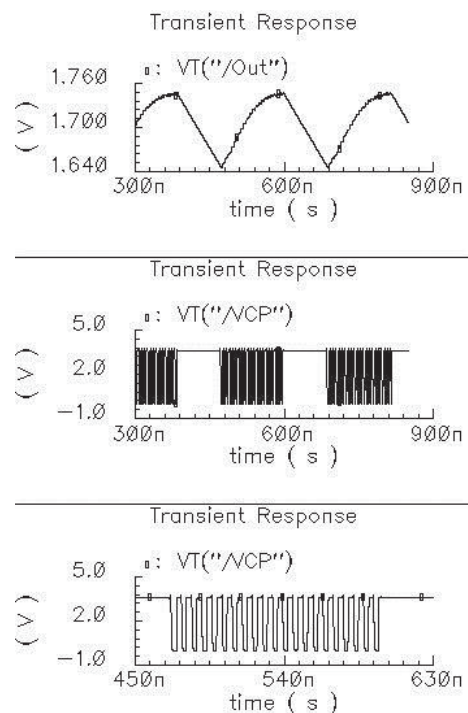


Fig. 9. The waveforms of  $V_{out}$  and  $V_{cp}$  when  $I_{Load}=5$  mA.

The waveforms of the output voltage  $V_{out}$  and control pulses of main power PMOS transistor, when the load current  $I_{Load}$  is equal to 5mA, are presented in Fig. 9. As it can be seen from the pictures shown in Fig. 8 and Fig. 9 the designed PFM controlled buck converter works in proper manner and the average value of the output voltage  $V_{out}$  is equal to 1.7V. The waveforms shown in Fig. 9 prove that at light load the system operates longer in sleep mode.

For the oscillator with fixed 50% duty-cycle is used ring oscillator. The schematic of this ring oscillator is shown in Fig. 10.

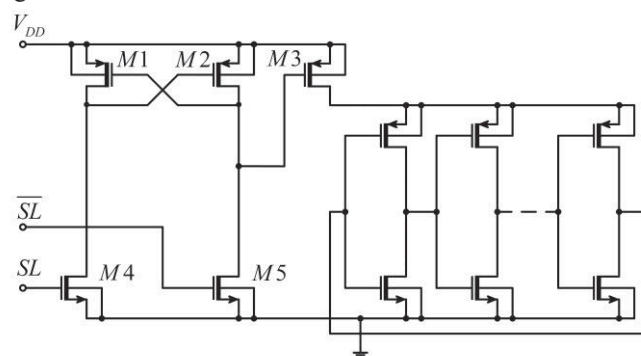


Fig. 10. Ring oscillator.

The power supply of this stage is switched-off in sleep mode in order to minimize the power losses in the PFM control system. Thus the overall efficiency of buck converter could be increased. If the output voltage of the buck converter  $V_{out}$  is higher than the desired voltage, the control signal “ $SL$ ” has high voltage level, while “ $\overline{SL}$ ” has low voltage level. In this case the transistor  $M3$ , which is illustrated in Fig. 10, is switched-

off. If  $V_{out}$  is smaller than the desired voltage, the control signal “ $SL$ ” has high voltage level and  $M3$  is switched-on.

The efficiency  $\eta$  results of the PFM controlled buck converter as a function of the load current  $I_{Load}$  are presented in Table II.

TABLE II  
PFM CONTROL  
EFFICIENCY OF BUCK CONVERTER AS A FUNCTION OF  $I_{Load}$

PFM Controlled Buck Converter	
$I_{Load}$ [mA]	Efficiency [%]
30	58
20	60
10	55
8	57
5	54.5
2	35
1	24

The efficiency results of PWM and PFM buck converter as a function of the load current  $I_{Load}$  are graphically presented in Fig. 11.

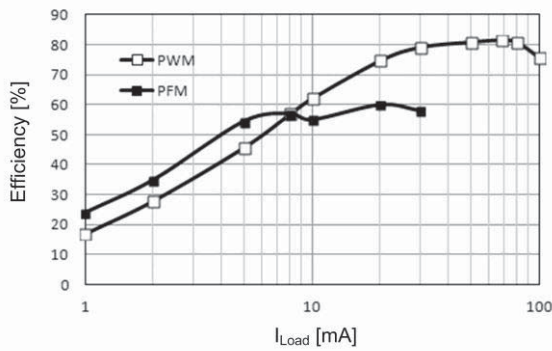


Fig. 11. Efficiency of PWM and PFM controlled buck converter as a function of  $I_{Load}$ .

The obtained results, illustrated in Fig. 11 and presented in Table I and Table II, show that the efficiency of the designed switching-mode regulator is higher at light loads if PFM control is used. If  $I_{Load}$  is higher than 8mA the PWM is more efficient control technique. When the load current is smaller than 8mA the efficiency of the PFM controlled buck converter is around 7% higher compared to the efficiency of the PWM controlled buck converter. The battery life of wearable electronic devices could be increased if PFM control for switching-mode regulator is used at light loads.

#### IV. CONCLUSION

Integrated PWM and PFM controlled buck converter designed for low power wearable electronic devices on CMOS 0.35  $\mu$ m technology has been proposed in this paper. The input voltage is equal to 3.6V and the output voltage is regulated to be equal to 1.7V. The maximum efficiency  $\eta$  of the buck converter is 81.43%, when the load current is equal to 68mA. When the load current  $I_{Load}$  is smaller than 8mA, the efficiency

of the PFM controlled buck converter is around 7% higher compared to the efficiency of the PWM controlled buck converter. The PFM control technique can increase the battery life of wearable electronic devices used in IoT system, because they operate over a long period of time at light load conditions.

#### ACKNOWLEDGEMENT

This work was supported by the European Regional Development Fund within the Operational Programme “Science and Education for Smart Growth 2014 - 2020” under the Project CoE “National center of mechatronics and clean technologies” BG05M2OP001-1.001-0008”, L2\_S1.

#### REFERENCES

- [1] C. Cheng, L. Lin, J. Lin, K. Chen, Y. Lin, J. R. Lin and T. Tsai, "A DVS-Based Burst Mode with Automatic Entrance Point Control Technique in DC-DC Boost Converter for Wearable Devices and IoT Applications", 2017 IEEE Asian Solid-State Circuits Conference (A-SSCC), Seoul, 2017, pp. 121-124.
- [2] A. Paidimarri and A. P. Chandrakasan, "A Wide Dynamic Range Buck Converter With Sub-nW Quiescent Power", IEEE Journal of Solid-State Circuits, vol. 52, no. 12, pp. 3119-3131, Dec. 2017.
- [3] N. Shafiee, S. Tewari, B. Calhoun and A. Shrivastava, "Infrastructure Circuits for Lifetime Improvement of Ultra-Low Power IoT Devices", IEEE Transactions on Circuits and Systems I: Regular Papers, vol. 64, no. 9, pp. 2598-2610, Sept. 2017.
- [4] A. Roy, A. Klinefelter, F. B. Yahya, X. Chen, L. P. Gonzalez-Guerrero, C. J. Lukas, D. A. Kamakshi, J. Boley, K. Craing, M. Faisal, S. Oh, N. E. Roberts, Y. Shakhshier, A. Shrivastava, D. P. Vasudevan, D. D. Wentzloff, and B. H. Calhoun, "A 6.45  $\mu$ W Self-Powered SoC with Integrated Energy-Harvesting Power Management and ULP Asymmetric Radios for Portable Biomedical Systems", IEEE Trans. Biomed. Circuits Syst., vol.9, no. 6 pp. 862-874, Dec. 2015.
- [5] Y. J. Park, J. H. Park, H. J. Kim, H. Ryu, S. Y. Kim, "A Design of a 92.4% Efficiency Triple Mode Control DC-DC Buck Converter With Low Power Retention Mode and Adaptive Zero Current Detector for IoT/Wearable Applications", IEEE Transactions on Power Electronics, vol. 32, no. 9, pp. 6946-6960, Sept. 2017.
- [6] M. Spasova, D. Nikolov, G. Angelov, R. Radonov, N. Hristov, "SRAM Design Based on Carbon Nanotube Field Effect Transistor's Model with Modified Parameters", 2017 40th International Spring Seminar on Electronics Technology (ISSE), pp. 1-4, 2017, Bulgaria.
- [7] Virtuoso Analog Design Environment, www.cadence.com.